Available online at www.sciencedirect.com

SciVerse ScienceDirect

Ceramics International 39 (2013) 7943–7949

CERAMICS INTERNATIONAL

www.elsevier.com/locate/ceramint

Effect of microstructure on cutting processability of porcelain tile subjected to different firing cycles

Shanjun Ke[a], Xiaosu Cheng[a,*], Yanmin Wang[a], Qianghong Wang[b], Zhidong Pan[a]

[a]College of Materials Science and Engineering, South China University of Technology, Guangzhou 510640, China
[b]Patent Examination Cooperation Center of SIPO, Guangzhou 510530, China

Received 4 March 2013; accepted 16 March 2013
Available online 23 March 2013

Abstract

The fast firing technique is one of the most important ways to save energy consumption and improve production efficiency in the porcelain tile industry. In the actual production, excessively short firing cycle time easily causes the cutting edge defects. This work examines the effect of microstructure on cutting processability of a representative composition of a commercial porcelain tile fired at 1200 °C with two different firing cycles as follows: 40 min and 60 min. The phase composition and microstructure were investigated by using a combination of techniques such as X-ray diffraction (XRD) and scanning electron microscopy (SEM). The result indicated that it was beneficial to extend firing cycle (from 40 min to 60 min) for the cutting processability of porcelain tiles, which was due to the formation of positive microstructures such as secondary mullite needles and small-volume residual quartz.

Keywords: A. Firing cycle; B. Microstucture; C. Porcelain tile; Roller kiln

1. Introduction

Porcelain tile is a vitreous ceramic product characterized by a low water absorption (usually less than 0.5%), with excellent technical properties such as compact microstructure, high mechanical strength, chemical and stain resistance [1–4]. These technical features make the porcelain tiles a popular product, whose production grows annually. Only in 2011, the output of all kinds of porcelain tiles has reached 8.5 billion square meters in China. However, ceramic tile industry is still at a high-energy-consumption and high-pollution level. Therefore, energy saving and emission reduction are both the burning questions for the ceramic tile industry.

A typical porcelain tile body is composed of 40–50% clay, 35–45% flux and 10–15% filler [5–8]. The clay as a binder confers plasticity on the green body for shaping and is usually kaolin and ball clay [5]. The flux is a low melting phase that lowers the temperature of liquid formation to obtain dense porcelain body at a relatively low temperature. Albite and potash feldspar are the most commonly used fluxes in porcelain [5,9]. The filler provides resistance to cracking during drying and forms a skeletal network during firing to mitigate pyroplastic deformation. Commercially, fillers used in porcelain bodies are often quartz sand, flint, alumina, and waste porcelain powders [8–10]. In order to reduce costs and protect environment, the low-grade mineral raw materials and some kinds of recycling wastes have been widely used in the production of porcelain tiles [11–19]. On the other hand, low-temperature and fast firing technique make the firing cycle of porcelain tile much shorter (40–90 min) than before (several hours) [8,9], which is one of the most important ways to save energy and reduce pollution emission. However, in order to save energy consumption and improve production efficiency, the firing cycle time is excessively shortened, which causes some product defects and quality issues such as undersintering, high water absorption and low strength [20].

Meanwhile, ceramic tile products must be processed further to meet dimensional tolerances and to enhance their artistic characteristics. Ceramic tiles can be machined by cutting and grinding. But porcelain tile is a brittle material, which easily cracks in the process of cutting. Recently, the cutting edge flaw defects of porcelain tiles were continually found in the actual production (Fig. 1). The aim of this work is to study the influence

*Corresponding author. Tel.: +86 20 87114217; fax: +86 20 87110273.
E-mail address: guangzhouscut@163.com (X. Cheng).

0272-8842/$ - see front matter © 2013 Elsevier Ltd and Techna Group S.r.l. All rights reserved.
http://dx.doi.org/10.1016/j.ceramint.2013.03.058

of microstructure on the cutting processability of porcelain tile. For this purpose, porcelain tile specimens with different microstructures were produced by varying the firing cycle time of ceramic roller kiln. The phase composition and microstructure of the products have been investigated by using a combination of techniques such as X-ray diffraction (XRD) and scanning electron microscopy (SEM).

2. Experimental procedure

2.1. Raw materials

Two kinds of clays, three kinds of quartz sands, two kinds of stone powders, bauxite and talcum were the starting raw materials, which were purchased by Foshan Ceramics Co., Ltd., China. The chemical compositions of raw materials are shown in Table 1.

2.2. Sample preparation

A formulation used for industrial production was selected as the experimental porcelain tile body composition (20 wt% clay, 24 wt% quartz sand, 38 wt% stone powder, 15 wt% bauxite and 3 wt% talcum). The Seger formulation of the experimental tile composition is given in Fig. 2.

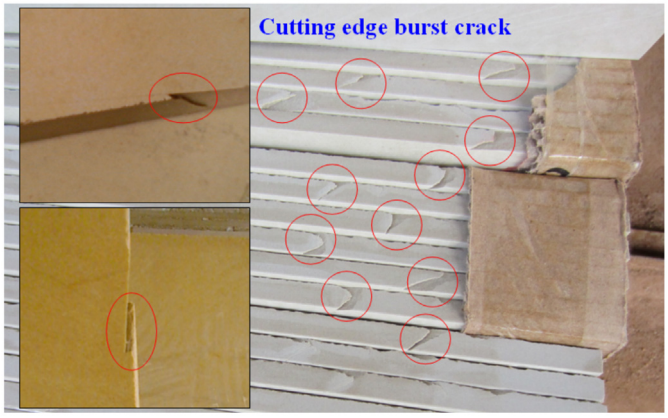

Fig. 1. Photograph of cutting edge flaw defects of porcelain tiles.

After batching, the raw materials, adding 0.5 wt.% polyethylene glycol (Guangzhou Taiqi Chemical Technology Co., Ltd., China) as a water reducing agent, they were wet milled in an industrial large-scale ball mill for 18 h. The slips were sieved by passing through a 250 mesh sieve and stored in a stirred storage tank, whose water content was about 32 wt%. Then, the slips were pumped from the stirred storage tank to a spray dryer. Spray drying was performed at temperatures ranging between 350 and 450 °C with a water content between 5% and 7% percent. The cuboid samples having $660 \times 660 \times 12\ mm^3$ size were shaped by a ceramic press machine (KD 3800, Guangdong KEDA Industrial Co., Ltd., China) with the maximum pressing force of 3800 kN. The pressed green bodies were polished and put into the roller dryer automatically. The highest drying temperature was less than 200 °C.

The dried green bodies were sintered at 1200 °Cin a ceramic roller kiln. The ceramic roller kiln is a new type of continuous industrial kiln, whose cross-section is long and narrow, and products are set on an array of parallel rollers which have high temperature and thrill through the working zone of the kiln [21]. It is mainly composed of the preheating zone, the firing zone and the cooling zone. Fig. 3 shows the schematic illustration of ceramic roller kiln. In this experiment, the roller kiln has 108 m length and 2.4 m width. The firing zone length is about 33 m and the natural gas is used as fuel in the ceramic roller kiln. To study the cutting edge flaw of porcelain tiles, the samples are subjected to two different firing cycles (40 min and 60 min), which are obtained easily by adjusting the operation speed of the production line. The temperature curve of the experimental roller kiln is shown in Fig. 4.

$$\{0.16\ K_2O,\ 0.23\ Na_2O,\ 0.04\ CaO,\ 0.16\ MgO\} \cdot \{0.97\ Al_2O_3,\ 0.03\ Fe_2O_3\} \cdot \{6.37\ SiO_2,\ 0.02\ TiO_2\}$$

Fig. 2. Seger formulation of the experimental tile composition.

Table 1
Chemical composition of raw materials.

Raw materials	Constituents (wt%)								
	SiO_2	Al_2O_3	Fe_2O_3	TiO_2	CaO	MgO	K_2O	Na_2O	Ignition loss
Clay-1	64.29	23.33	1.07	0.54	0.26	0.34	2.81	0.25	7.47
Clay-2	56.17	28.36	2.68	1.28	0.01	0.24	0.69	0.37	10.31
Bauxite	49.01	33.94	1.51	2.02	0.02	0.15	1.40	0.91	11.44
Talcum	53.96	2.63	0.74	0.21	2.42	27.57	0.16	0.32	11.99
Quartz sand-1	75.13	15.90	0.64	0.01	0.04	0.18	2.61	3.58	1.66
Quartz sand-2	72.35	16.53	0.69	0.10	0.23	0.19	5.11	3.10	2.18
Quartz sand-3	69.44	18.29	0.78	0.40	0.14	0.43	3.06	5.58	1.31
Stone powder-1	71.26	17.49	1.30	0.07	0.04	0.21	4.69	0.53	3.44
Stone powder-2	68.22	23.56	1.33	1.20	0.02	0.77	3.26	0.41	1.23

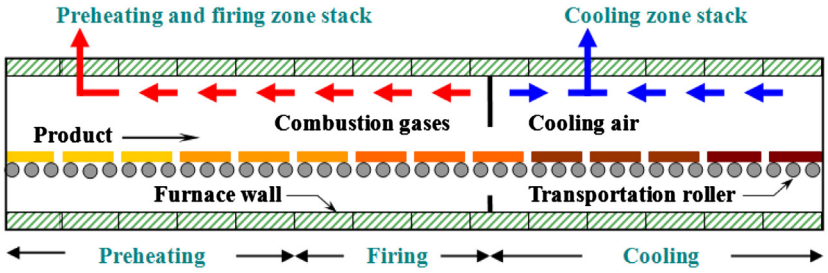

Fig. 3. Schematic illustration of ceramic roller kiln.

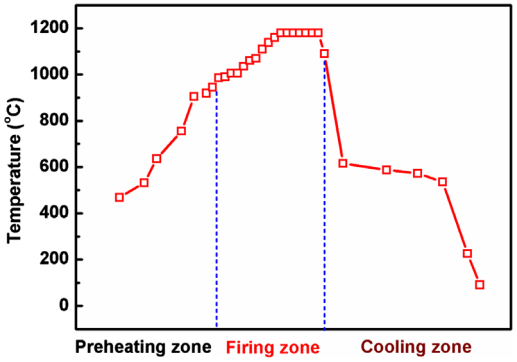

Fig. 4. Temperature curve of experimental ceramic roller kiln.

Table 2
Damage rate of the test samples with different firing cycles.

Sample	Firing cycle (min)	Number of samples	Number of damage samples	Damage rate (%)
A	40	150	56	37.3
B	60	150	4	2.7

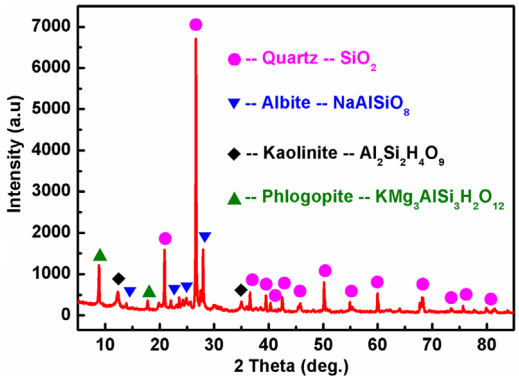

Fig. 5. XRD pattern of sample unfired.

2.3. Measurements and analyses

The crystalline phases were determined by an X-ray diffractometer (XRD, Philips PW-1710, the Netherlands) using Cu *Kα* radiation. The microstructure morphology of the sintered samples, which were polished and coated with gold–palladium, was observed by scanning electron microscopy (SEM, Philips L30FEG, the Netherlands). And microanalysis was also performed using the embedded energy dispersive spectrometer (EDS) digital controller and control software.

3. Results and discussion

3.1. Cutting processability

In order to make a statistical analysis, 300 samples were chosen in the experimental process. There are 150 test samples fired at 1200 °C with a firing cycle of 40 min, the other 150 test samples fired at 1200 °C for 60 min. All fired samples were machined by cutting into $600 \times 600\ mm^2$ dimensions. The number of damage samples (existence of cutting edge flaw defects) was counted and the damage rate of test samples was calculated and shown in Table 2. As seen from the table, the damage rate of test samples reaches 37.3%, when the firing cycle is 40 min. By increasing the firing cycle to 60 min, the damage rate drops to 2.7%. The result indicated that it was beneficial to extend firing cycle (from 40 min to 60 min) for the cutting processability of the porcelain tile.

The cutting edge flaw is related to brittleness of ceramic material which fails in a brittle manner. As is known to all, brittleness is a vital weakness of ceramic material, which can be quantitatively described by fracture toughness (K_{IC}). On the basis of elastic fracture mechanics, fracture toughness can be associated with the fracture energy (γ_i) and Young's modulus (E) by equation:

$$K_{IC} = \sqrt{2E\gamma_i} \quad (1)$$

where E is the Young's modulus; and γ_i the fracture energy of the material, they are supposed to be positively correlated [22,23]. The equation determines that the fracture toughness of a ceramic material can be characterized by two factors: Young's modulus and the fracture energy. An increase in fracture toughness of ceramic materials can be achieved by increasing the ratio of crystalline to glassy phase. Besides an increase in crystallinity, crack deflection, i.e., propagation of crack front around grains and second phase formation is the main mechanism that contributes to an increase in fracture toughness [24]. Therefore, it was reported by several authors that alumina, cristobalite and mullite as the second phase in porcelain ceramics toughen the fired body [9,25,26].

3.2. Phase analysis

Fig. 5 shows X-ray diffraction (XRD) pattern of the green body. The analysis result indicated that quartz was the major phase in the unfired samples with a little proportion of albite and phlogopite, and a small amount of kaolinite. When the green bodies were heated at high temperatures, the crystalline phase compositions had a significant change. Fig. 6 shows XRD patterns of the samples fired at 1200 °C with different firing cycles. The firing cycle of sample A is 40 min, 60 min for sample B. Quartz was the only mineral phase existing in the green body and detected in the fired products. All the other mineral phases existing in the green body have disappeared, being replaced by mullite and glassy phase. On curves A and B, quartz peaks are far stronger than mullite peaks which means quartz is the dominant crystalline phase, while the amount of mullite is very small. Compared with two curves (Fig. 6), the quartz phase content decreases and mullite phase content increases with increasing the firing cycle (from 40 min to 60 min). This was due to both mullite crystallization and quartz dissolution in the liquid phase, when the firing cycle was extended. Formation of mullite in porcelain bodies has been extensively studied by many literatures [27,28].

According to a mixture law, it is possible to calculate Young's modulus (E) of ceramic materials if no cracks were present. The E of ceramic materials can be roughly evaluated by the following equation:

$$E = E_i V_i + E_m V_m \quad (2)$$

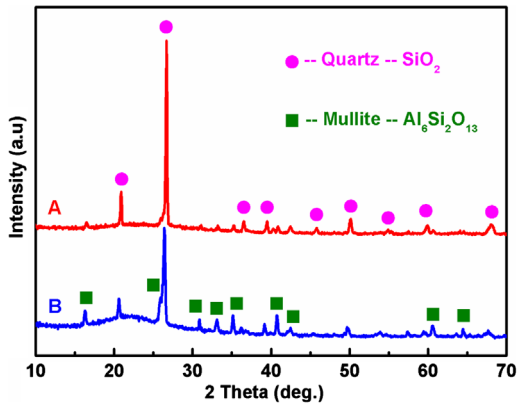

Fig. 6. XRD patterns of samples fired at 1200 °C with different firing cycles, (A) 40 min and (B) 60 min.

where E, E_i and E_m represent Young's modulus of ceramic material, i-phase and matrix, V_i and V_m stand for volume fractions of i-phase and matrix [29]. Mullite is a high-strength material. Young's modulus of pure mullite ceramic can reach ~220 GPa [30]. According to Fig. 6, which shows that the mullite in sample B is more than in sample A, the E value of sample B is also higher than that of sample A. So, sample B has higher fracture toughness and lower brittleness, which is not prone to develop the cutting cracks on the edge of porcelain tiles.

3.3. Microstructure analysis

The difference found in the cutting processability of porcelain tile cannot be explained only on the basis of the phase composition, a careful microstructural analysis was carried out. Fig. 7 shows SEM micrographs of the polished surface of samples fired at 1200 °C with different firing cycles. Sample A contains both isolated large pores and generally interconnected fine pores in large numbers, which are less spherical (elongated or ellipsoid). Sample B is slightly more compact in comparison with sample A, which is characterized by the presence of large smooth areas, in which isolated round pores are embedded. The pore size distribution is rather wide, and pores of about 50 μm in size are also present. With the extension of firing cycle, a larger development of liquid phase is able to decrease porosity and transform interconnected pores into spherical ones. Dean and Lopez [31] observed a linear decrease of Young's modulus with the increase in porosity according to the linear relationship:

$$E_p = E_0(1-\varepsilon P) \quad (3)$$

where E_0 is Young's modulus of pore-free material, ε is an empirical constant and P is the volume fraction of pores. So, the decrease in porosity with increasing firing cycle (from 40 min to 60 min) is beneficial to toughen the fired porcelain tiles.

Fig. 8 shows SEM micrographs of mullite in the porcelain tiles fired at 1200 °C with different firing cycles. As clearly shown, the mullite morphology exhibits different microstructures dependences on the firing cycle. Microstructure of the mullite fired at 1200 °C for 40 min (Fig. 8A) is characterized by the formation of aggregate and micropores, which is generally referred to as primary mullite and derives from the pure clay agglomerate relicts [5]. When the firing cycle is

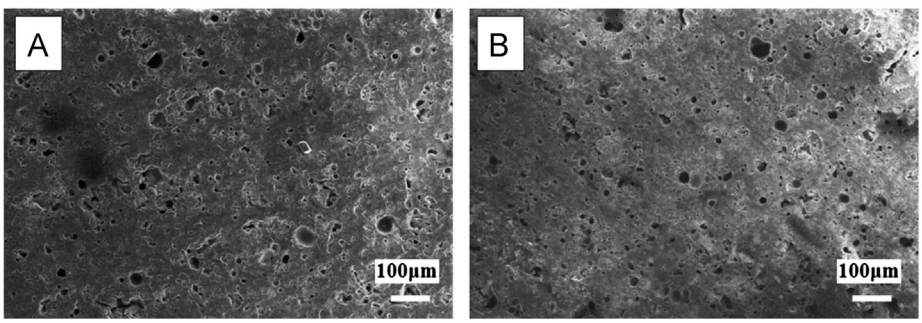

Fig. 7. Pore structures of samples fired at 1200 °C with different firing cycles, (A) 40 min and (B) 60 min.

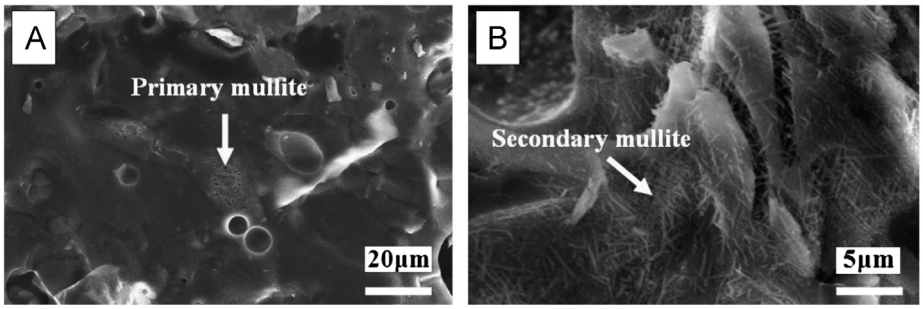

Fig. 8. SEM micrographs of mullite in the porcelain tiles fired at 1200 °C with different firing cycles, (A) 40 min and (B) 60 min.

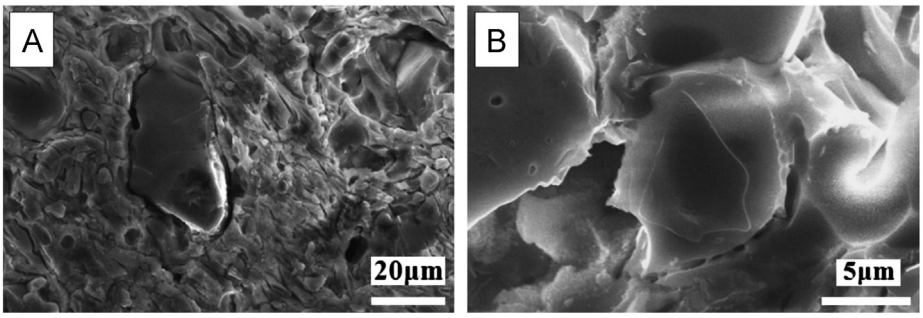

Fig. 9. SEM micrographs of quartz in the porcelain tiles fired at 1200 °C with different firing cycles, (A) 40 min and (B) 60 min.

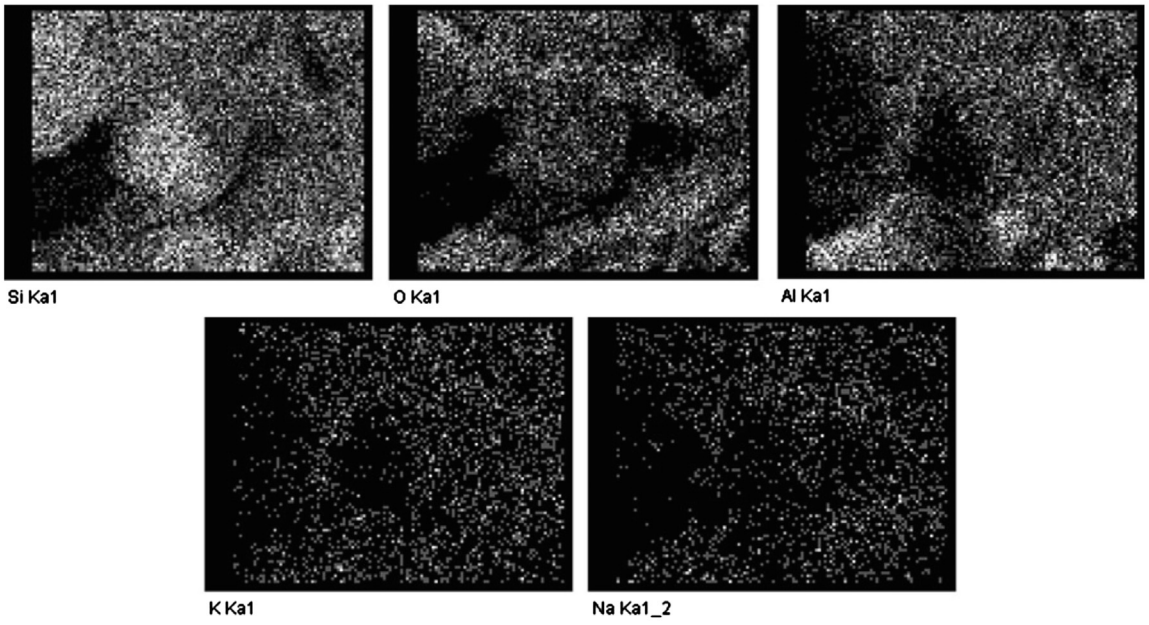

Fig. 10. EDS analysis of the investigated sample B in Fig. 9B.

extended to 60 min, sample B shows a large amount of elongated needle-shaped mullite in Fig. 8B, which is termed secondary mullite. Early study [32] revealed secondary mullite does not form from pure feldspar relicts since these contain insufficient alumina but from feldspar penetrated clay relicts or mixtures of fine clay, quartz and feldspar.

One of the oldest theories on the strength of porcelain, the mullite hypothesis [9,10], suggests that porcelain strength depends on the felt-like interlocking of fine mullite needles. Specifically, the higher the mullite content and higher the interlocking of the mullite needles, the higher is the strength. Hence, secondary mullite, because of its acicular morphology and smaller needle diameter, could be more favorable to increase strength than primary mullite [9]. Furthermore, fibrous mullite distributed in the glass matrix grows a three-dimensional network, which can lead to significantly increased macroscopic strength and toughness of ceramic materials [33]. As the firing cycle increased from 40 min to 60 min, a large

number of secondary mullite are formed, which enhanced the impact resistance of porcelain tile.

Fig. 9 shows SEM micrographs of quartz in the porcelain tiles fired at 1200 °C with different firing cycles. The morphology of residual quartz grain can be seen clearly from Fig. 9. On the basis of Figs. 9B and 10, sample B exhibits approximately triangular quartz grain. Meanwhile, sample A presents some microcracks between the unsolved quartz particle and matrix, whereas the quartz particle in sample B is completely surrounded and aligned with a large number of glassy matrix. Generation of microcracks is attributed to the difference between the coefficients of thermal expansion of the quartz and glassy matrix, developing microscopic residual stress [23,24,34]. When the residual stress increases with the increase of quartz particle size, it may even lead to quartz particle detachment from the glassy matrix, as seen in Fig. 9A. This microstructural damage adversely affects the porcelain tile's cutting processability. Previous research [20,35,36] also indicated that the process of quartz particle detachment from the matrix is encouraged by the anisotropic behavior of quartz under thermal expansion. The diameter of the residual quartz is about 40 μm in sample A and 8 μm in sample B. That is, existence of the large-volume residual quartz leads to microscopic residual stress, which make the porcelain tiles relatively unstable and thus easily develop cracks, as porcelain tiles are machined by cutting.

4. Conclusions

A mixture of 20 wt% clay, 24 wt% quartz sand, 38 wt% stone powder, 15 wt% bauxite and 3 wt% talcum was selected as representative composition of commercial porcelain tiles subjected to two different firing cycles: 40 min and 60 min. The change in firing cycles resulted in the differences of the cutting processability and microstructure of the products. The damage rate of porcelain tile reached 37.3%, when the firing cycle was 40 min. With increasing the firing cycle to 60 min, the damage rate dropped to 2.7%. The cutting processability was closely related to the phase composition and microstructure of porcelain tile. An increase in mullite content was observed to decrease quartz content with increasing the firing cycle. The quartz particle detached from the matrix when the particle size of residual quartz was about 40 μm. The existence of secondary mullite needles and small-volume residual quartz were beneficial to enhance the impact resistance of porcelain tile.

Acknowledgments

This work was supported by the Major Scientific and Technological Projects of Guangdong Province (No. 2010A080804001) and the ChanXueYan Special Funds of Guangdong (Nos. 2011B090400201 and 2012B091100306).

References

[1] Kr.D. Swapan, D. Kausik, Differences in densification behavior of K- and Na- feldspar-containing porcelain bodies, Thermochimica Acta 406 (2003) 199–206.
[2] X.S. Cheng, S.J. Ke, Q.H. Wang, H. Wang, A.Z. Shui, P.A. Liu, Characterization of transparent glaze for single-crystalline anorthite, Ceramics International 38 (2012) 4901–4908.
[3] J.L. Amoros, M.J. Orts, J. Garcia-Ten, A. Gozalbo, E. Sanchez, Effect of the green porous texture on porcelain tile properties, Journal of the European Ceramic Society 27 (2007) 2295–2301.
[4] D.Y. Tuncel, E. Ozel, Evaluation of pyroplastic deformation in sanitary-ware porcelain bodies, Ceramics International 38 (2012) 1399–1407.
[5] W.E. Lee, Y. Iqbal, Influence of mixing on mullite formation in porcelain, Journal of the European Ceramic Society 21 (2001) 2583–2586.
[6] J. Martín-Márquez, J.M. Rincón, M. Romero, Mullite development on firing in porcelain stoneware bodies, Journal of the European Ceramic Society 30 (2010) 1599–1607.
[7] A. Capoglu, A novel low-clay translucent whiteware based on anorthite, Journal of the European Ceramic Society 31 (2010) 321–329.
[8] J. Martín-Márquez, J.M. Rincón, M. Romero, Effect of firing temperature on sintering of porcelain stoneware tiles, Ceramics International 34 (2008) 1867–1873.
[9] U. Senapati, W.M. Carty, Porcelain-raw materials, processing, phase evolution, and mechanical behavior, Journal of the American Ceramic Society 81 (1998) 3–20.
[10] G. Stathis, A. Ekonomakou, C.J. Stournaras, C. Ftikos, Effect of firing conditions, filler grain size and quartz content on bending strength and physical properties of sanitaryware porcelain, Journal of the European Ceramic Society 24 (2004) 2357–2366.
[11] E. Rambaldi, L. Esposito, A. Tucci, G. Timellini, Recycling of polishing porcelain stoneware residues in ceramic tiles, Journal of the European Ceramic Society 27 (2007) 3509–3515.
[12] B. Karasu, M. Caki, Y.G. Yesilbas, The effect of albite wastes on glaze properties and microstructure of soft porcelain zinc crystal glazes, Journal of the European Ceramic Society 21 (2001) 1131–1138.
[13] R.C. Da Silva, S.A. Pianaro, S.M. Tebcherani, Preparation and characterization of glazes from combinations of different industrial wastes, Ceramics International 38 (2012) 2725–2731.
[14] C. Sikalidis, V. Zaspalis, Utilization of Mn–Fe solid wastes from electrolytic MnO_2 production in the manufacture of ceramic building products, Construction and Building Materials 21 (2007) 1061–1068.
[15] C.M.F. Vieira, P.M. Andrade, G.S. Maciel, F. Vernilli Jr., S.N. Monteiro, Incorporation of fine steel sludge waste into red ceramic, Materials Science and Engineering A 427 (2006) 142–147.
[16] R.R. Menezes, H.G. Malzac Neto, L.N.L. Santana, H.L. Lira, H.S. Ferreira, G.A. Neves, Optimization of wastes content in ceramic tiles using statistical design of mixture experiments, Journal of the European Ceramic Society 28 (2008) 3027–3039.
[17] M. Hojamberdiev, A. Eminov, Y.H. Xu, Utilization of muscovite granite waste in the manufacture of ceramic tiles, Ceramics International 37 (2011) 871–876.
[18] R.R. Menezes, H.S. Ferreira, G.A. Neves, H.L. de Lira, H.C. Ferreira, Use of granite sawing wastes in the production of ceramic bricks and tiles, Journal of the European Ceramic Society 25 (2005) 1149–1158.
[19] A. Christogerou, T. Kavas, Y. Pontikes, S. Koyas, Y. Tabak, G.N. Angelopoulos, Use of boron wastes in the production of heavy clay ceramics, Ceramics International 35 (2009) 447–452.
[20] A.N. de Junior, D. Hotza, V.C. Soler, E.S. Vilches, Effect of quartz particle size on the mechanical behavior of porcelain tile subjected to different cooling rates, Journal of the European Ceramic Society 29 (2009) 1039–1046.
[21] M. Chmielowski, E. Specht, Modelling of the heat transfer of transport rollers in kilns, Applied Thermal Engineering 26 (2006) 736–744.

[22] K. Hamano, Y.H. Wu, Z. Nakagawa, M. Hasegawa, Effect of coarse quartz grain on mechanical strength of porcelain body, Journal of the Ceramic Society of Japan International Edition 99 (1991) 1070–1073.
[23] K. Hamano, Y.H. Wu, Z. Nakagawa, M. Hasegawa, Effect of grain size of quartz on mechanical strength of porcelain bodies, Journal of the Ceramic Society of Japan International Edition 99 (1991) 149–153.
[24] C.B. Ustundag, Y.K. Tur, A. Capoglu, Mechanical behavior of a low-clay translucent whiteware, Journal of the European Ceramic Society 26 (2006) 169–177.
[25] R. Harada, N. Sugiyama, H. Ishida, Al_2O_3-strengthened felds-pathic porcelain bodies: effects of the amount and particle size of alumina, Ceramic Engineering and Science Proceedings 17 (1996) 88–98.
[26] W.P. Tai, K. Kimura, K. Jinnai, A new approach to anorthite porcelain bodies using nonplastic raw materials, Journal of the European Ceramic Society 22 (2002) 463–470.
[27] H. Schneider, J. Schreuer, B. Hildmann, Structure and properties of mullite-A review, Journal of the European Ceramic Society 28 (2008) 329–344.
[28] W.E. Lee, G.P. Souza, C.J. McConville, T. Tarvornpanich, Y. Iqbal, Mullite formation in clays and clay-derived vitreous ceramics, Journal of the European Ceramic Society 28 (2008) 465–471.
[29] A.P.N. de Oliveira, E.S. Vilches, V.C. Soler, F.A.G. Villegas, Relationship between Young's modulus and temperature in porcelain tiles, Journal of the European Ceramic Society 32 (2012) 2853–2858.
[30] E. Zadeh Hayati, O. Mohammad Moradi, M. Ghassemi Kakroudi, Investigation of the effect of sintering temperature on Young's modulus evaluation and thermal shock behavior of a cordierite-mullite based composite, Materials and Design 45 (2013) 571–575.
[31] E.A. Dean, J.A. Lopez, Empirical dependence of elastic moduli on porosity for ceramic materials, Journal of the American Ceramic Society 66 (1983) 366–370.
[32] Y. Iqbal, W.E. Lee, Microstructural evolution in triaxial porcelain, Journal of the American Ceramic Society 83 (2000) 3121–3127.
[33] K. Boussois, N. Tessier-Doyen, P. Blanchart, Anisotropic kinetic of the kaolinite to mullite reaction sequence in multilayer ceramics, Journal of the European Ceramic Society 33 (2013) 243–249.
[34] A. De Noni Jr., D. Hotza, V. Cantavella, E. Sánchez, Influence of macroscopic residual stresses on the mechanical behavior and microstructure of porcelain tile, Journal of the European Ceramic Society 28 (2008) 2463–2469.
[35] S.R. Braganca, C.P. Bergmann, H. Hübner, Effect of quartz particle size on the strength of triaxial porcelain, Journal of the European Ceramic Society 26 (2006) 3761–3768.
[36] A. De Noni Jr., D. Hotza, V. Cantavella, E. Sánchez, Analysis of the development of microscopic residual stresses on quartz particles in porcelain tile, Journal of the European Ceramic Society 28 (2008) 2629–2637.